Toner Adhesion State Control in Electrophotography

Christopher A. DiRubio, Palghat Ramesh, Aaron M. Burry, and Antonio DeCrescentis; Xerox Corporation, Webster NY

1. Abstract

In electrophotographic (xerographic) marking systems the toner adhesion state impacts development, transfer, cleaning, and toner transport. The adhesion state can be linked to critical to customer responses (CTCs) like color consistency and stability, color macro-uniformity, color accuracy and gamut, and image noise and mottle. In this paper we will discuss the key control factors that impact the toner adhesion state and provide specific examples of how the toner adhesion state may be optimized through improved toner design (materials) and closed loop feedback and control (hardware and controls) within xerographic engines [1]. The linkage between toner adhesion state control factors and the CTCs is illustrated in the process diagram in figure 1. Improved control of the toner adhesion state may be enabling for expanded media latitude and 6 to 8 color tandem intermediate belt xerography.

We have measured and simulated the electric field detachment distributions of toners with differing properties to improve our understanding of how the key control factors and their distributions impact adhesion and toner detachment. Monte-Carlo simulations using extensions of the adhesion models developed by James Feng and Dan Hays have proved particularly helpful in interpreting the measured detachment field distributions, quantifying how the control factors (mean and variance) impact these distributions, and improving our fundamental understanding of the electric field detachment of toner.

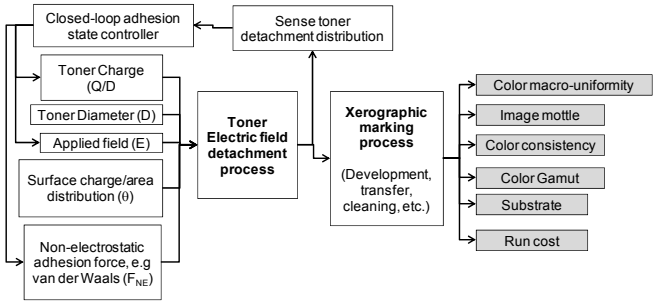

Figure 1 Toner State Control process flow diagram

2. Results and observations

A measured detachment field distribution is illustrated in figure 2 for conventional mechanically ground toner with a tribocharge of Q/M = 37μC/g. Toner was developed to a photoreceptor surface and then transferred to a tuned conductivity intermediate transfer belt (ITB) over a range of electric fields in a commercial printer (Xerox DC12) . The percentage of the toner mass per unit area (RMA = Residual Mass per unit Area) remaining on the photoreceptor after passing through the high field transfer nip region was measured at each applied transfer field. The transfer field was varied from roughly 0 V/μm to fields exceeding the nominal value of roughly 60 V/μm used during normal print operation.

The peak applied transfer field is estimated based on a Biased Transfer Roll (BTR) electric field nip model that accounts for a host of control factors including the voltage applied to the BTR shaft, the surface potential of the photoreceptor, BTR & ITB resistivity and dielectric thickness, charge deposition on the ITB and photoreceptor surfaces due to air breakdown, toner pile height and charge, process speed, etc. The model may (from Gauss's law) overestimate the transfer field [V/μm] by as much as 1.13*(Q/M)*(M/A)*(1-RMA/100), where Q/M the toner charge in μC/g, M/A is the toner mass per unit area on the photoreceptor prior to the application of the transfer field in the nip (M/A ~ 0.45 to 0.5 mg/cm^2 in these experiments), and RMA is the fraction of toner that has transferred to the image receiving substrate at a given field. We chose not to include this Gauss's law correction to the model because it may not be applicable since transfer occurs across very small air gaps that are on the order of the diameter of a toner particle. Therefore, the expression above gives an upper bound in the overestimate of the field.

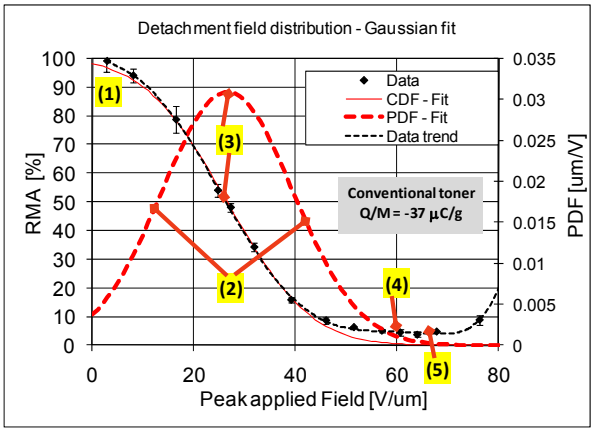

Figure 2 Measured detachment field distribution for conventional toner

The solid red line is a Gaussian fit to CDF(E) = 100% - RMA(E), where RMA(E) is the measured RMA (black points), and the CDF(E) is the cumulative distribution function for a Gaussian distribution. The Gaussian PDF (Probability Density Function, i.e. the bell shaped curve/histogram representing the detachment field distribution) corresponding the CDF is plotted as a dashed red line. There are several features of this curve worth noting. The detachment field distribution is extremely broad (see (2) in figure 2), and includes some toners that detach at very low fields. Toners that detach at fields less than 3 V/μm (see (1))can lead to image noise and blur due gap transfer prior to the establishment of intimate contact between the substrate (Intermediate Transfer Belt) and image bearing member (photoreceptor). The mean detachment field for the toner is about

26 V/µm (3) and most of the toner (~96%) has detached below 55 V/um. Between 55 and 70 V/µm there is a flat region (5) representing about 4% of the toner. This toner belongs to a sub-population of "un-detachable toner" that does not detach despite the increasing transfer field.

The un-detachable sub-population of toner can be understood by examining the net force on a toner particle. This force can be represented by the following equation from the Feng-Hays adhesion model [2-4]:

$$F_{Toner} = (\beta)QE - (\alpha)\frac{Q^2}{16\pi R^2 \varepsilon_0} - (\gamma)\pi\varepsilon_0 R^2 E^2 - F_{NE} \quad (1)$$

Where F_{Toner} is the net force on the toner, βQE is the Lorentz pull-off force due to the applied field (E), the second term is the image force adhesion, the third term represents the adhesion due to the dipole moment induced by the applied field, and the final term represents non-electrostatic adhesion forces like the van der Waals force. The α, β, γ terms in the equation account for multipole interactions and θ, the uniformity of the charge distribution on the toner particle [2-4]. The parameter θ is also illustrated in figure 5.

The net force on conventional toner is plotted in figure 3 for different values of Q/M (Tribocharge) in units of µC/g. The distribution of the charge on the toner particle surface was assumed to be highly non-uniform with a polar half angle of θ = 10° (see figure 5). A toner will only detach if the pulloff force exceeds the adhesion, i.e. the net force (F_{Toner}) is greater than 0. At a Q/M of -40 µC/g (red curve) the toner detaches at a field of about 46 V/um, well below the nominal peak nip field of ~ 60 V/µm. The net force on low charge toner, however, never becomes positive at any applied field, so these low charge toners contribute to the un-detachable sub-population. This is illustrated in figure 3 by the curves for Q/M = -15 and -5 µC/g.

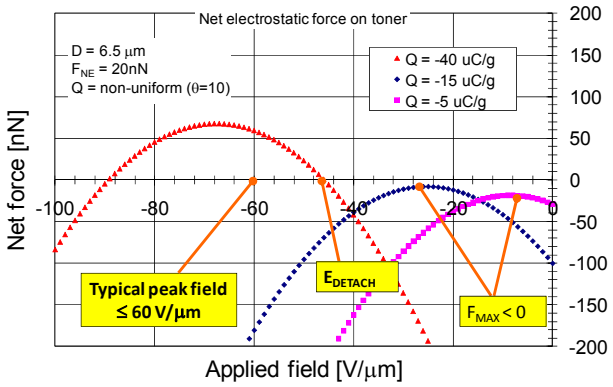

Figure 3 net force on a toner particle

Why is it that EA toners have higher transfer efficiency (lower residual mass per unit area (RMA)) at typical nominal peak transfer fields? We investigated this by measuring the detachment field distributions for chemically grown potato- and sphere-shaped EA (emulsion aggregate) toners with properties similar to the conventionally ground toner (see table 1). The PDFs extracted from the experimental results are shown in figure 4. Note that the mean detachment distributions for the EA potatoes (Blue) and EA spheres (red) with Q/M similar to conventional (black) had nearly the same mean detachment field and width. The RMA(E) at a nominal peak transfer field of 60 V/µm was, however, only 0.6% and 0.2 % for the EA potatoes and spheres respectively, well below the 3.6% observed for conventional toner. The EA toners had a lower fraction of un-detachable toners, not a lower mean detachment field. At a Q/M of 57 µC/g the EA spheres detachment field distribution had a significantly higher mean detachment field but a narrower width, indicating that a closed loop controller that varied the Q/M (tribocharge) could be used to minimize the mean detachment field. Closed-loop control schemes like this are described in detail in a recent patent application [1].

Table 1 Toner properties

	Conventional	EA spheres	EA spheres	EA potatoes
<d> [um]	6.1	5	5	5.94
Q/M [uC/g]	-37	-39	-57	-38
Q/D [fC/um]	-0.89	-0.54	-0.78	-0.74
<Q> [fC]	-5.5	-2.7	-3.9	-4.4
ρ [kg/m^3]	1240	1050	1050	1050

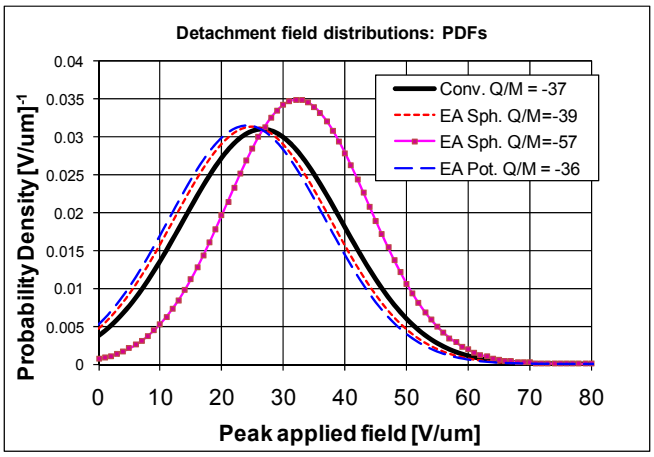

Figure 4 toner comparisons from measurements

3. Results from simulations

In order to improve our understanding of how toner properties impact the detachment field distributions, we have conducted Monte-Carlo simulations based in the Feng-Hays adhesion model shown in equation (1). The detachment field and maximum applied force, which are illustrated in figure, are given by the following expressions derived from equation (1):

$$E_{DETACH} = \frac{\beta Q}{2\gamma\pi\varepsilon_0 R^2} + \sqrt{\left(\frac{\beta Q}{2\gamma\pi\varepsilon_0 R^2}\right)^2 - \frac{\frac{\alpha Q^2}{16\pi\varepsilon_0 R^2} + F_{NE}}{\gamma\pi\varepsilon_0 R^2}} \quad (2)$$

, and

$$F_{MAX} = \frac{(4\beta^2 - \alpha\gamma)Q^2}{16\gamma\pi\varepsilon_0 R^2} - F_{NE} \quad (3)$$

The detachment field is only meaningful when F_{MAX}, the peak F_{TONER} (eq. (1)), satisfies $F_{MAX} > 0$. When this rule is violated, F_{TONER} is < 0 at all applied fields and the toner is therefore considered "un-detachable". As is illustrated in Figure 2, most of the measured residual mass observed at the nominal transfer field of 60 V/μm for conventional toner is due to un-detachable toner that cannot be removed even at the highest applied fields.

In the first set of simulations an attempt was made to reproduce the detachment field distribution for conventional toner observed in figure 2. At best we would expect qualitative agreement with the data due to limitations in the model. These limitations include the assumption of isolated non-interacting toner particles (no dependence of the force on area coverage, etc.), a conducting (as opposed to dielectric) photoreceptor surface, toner surface charge confined to the polar caps of a spherical toner particle, no toner charge modification within the nip, etc. A full accounting of the limitations is beyond the scope of this paper, but keep in mind that despite the imperfections in the model we can still reasonably expect to gain insight into how basic toner properties impact the detachment field distributions.

The input factors used in the conventional toner simulation are summarized in table 2 (compare to table 1). They include: (1) F_{NE} [nN] , the non-electrostatic contribution to adhesion (van der Waals, etc.), (2) R [μm], the radius of the toner, (3) Q/D [fC/μm], the charge to toner diameter ratio (D=2*R), and (4) the surface charge uniformity parameterized as θ , which defines the polar half cap angle containing the charge. In order to better understand θ, consider figure 5. A uniformly charged toner particle corresponds to θ = 90, and a highly non-uniformly charged particle may, for example, have θ <=20, with all of the toner Q concentrated near the "north" and "south" poles. Note that Q, the total toner charge, is given by Q = (Q/D)*D.

The means and standard deviations of the distributions of input parameters are shown in Table 2. The Q/D and R distributions were determined from charge spectrographs and tribo (Q/M) measurements. The charge spectrographs were measured from toner developed to the photoconductor. See table 3 for a conversion of Q/D to tribo. The actual R distribution had a long, large-particle tail that was not adequately captured by a normal distribution, but for simplicity we decided to use a Gaussian distribution anyway. The choice of the 1 um standard deviation was based estimated from the measured distribution.

Neither the charge uniformity (θ) nor the magnitude of the non-electrostatic adhesion (F_{NE}) was known for the conventional toner. Therefore both parameters were varied in the simulations to find a combination of F_{NE} and θ that reproduced the experimentally determined mean detachment field of ~26 V/μm and roughly reproduced the observed fraction of un-detachable toner. The parameters chosen for the simulation gave reasonable values for the magnitudes of F_{NE} and θ [4]. Note that Feng and Hays [2-4] only calculated α, β, and γ for three special cases: θ = 10, 20, and 90. Curve fitting was used determine α, β, and γ as a function of θ for $10^o < \theta < 90^o$.

The simulated detachment field distribution for conventional toner with a nominal Q/D ~ -0.9 fC/μm is illustrated in figure 6. A comparison to the measured distribution in figure 2 shows remarkable agreement considering the limitations of the model.

Table 2 Input parameters for conventional toner simulation. The first parameter is the mean, the second is the standard deviation.

Process Inputs			
Factor	Distro	First Parameter	Second Parameter
Theta	Normal	30	5
R	Normal	3.1	1
FNE	Normal	120	10
Q/D	Normal	-0.9	0.12

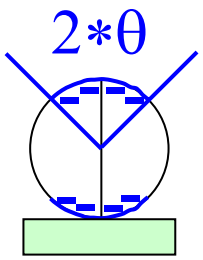

Figure 5 Toner surface charge uniformity parameter, θ, used in the simulations

The median detachment field in the simulation is 24 V/μm, which is in close agreement with the measured distribution (PDF in figure 6). The fraction of undetachable toners, however, is 19.5% in the simulation but only 3.6% in the experiments. In the simulation 2.6% of the toner detaches at fields greater than the nominal peak transfer field of 60 V/μm, compared to ~ 0% for the measurements. Therefore the overall residual at 60V/μm in the simulation is 22.1% (=19.5% + 2.6%) which is considerably higher than the 3.6% observed experimentally. The discrepancy may be due to the fact that the experiments were conducted with a DMA of ~ 0.5 mg/cm^2, which corresponds to over a monolayer of toner, whereas the simulations are only valid in the low area coverage

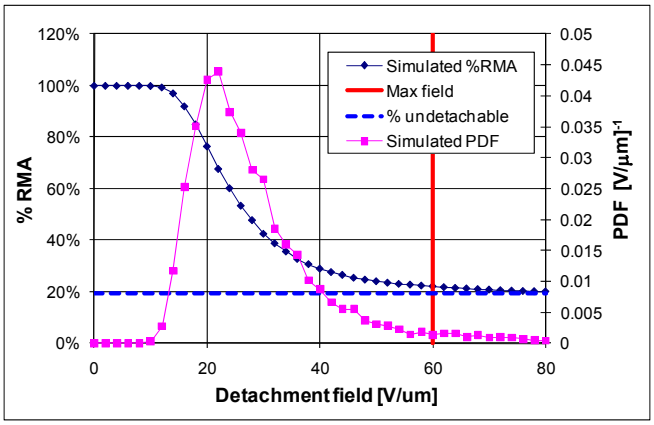

Figure 6 simulated detachment field distribution for conventional toner

limit of isolated non-interacting toner particles. The RMA at low DMA is closer to 70% according to unpublished data [5].

A Design of Experiments (DOE) approach utilizing a 4-factor 3-level Central Composite Design (CCD) was conducted to determine the impact of the control factors (table 2) on various aspects of the detachment field distribution. The responses included the fraction of un-detachable toner, the fraction of toner that only detaches above the peak nominal field of 60 V/μm, the mean detachment field, and others. While a full discussion of the results is beyond the scope of this paper, the impact of toner charge, Q/D, is illustrated in figure 7 and table 3.

The %RMA as a function of field is plotted in figure 7 as a function of Q/D for -1.3 <= Q/D <= -0.3 fC/μm (Tribo from ~ -12 to -60 μC/g). The simulations (see table 2 for input parameters) show that the fraction of un-detachable toner is a particularly strong function of Q/D, whereas the mean detachment field is only weakly dependent on Q/D. At low toner charge (Q/D = -0.3), 100% of the toner is un-detachable, whereas at a high toner charge of Q/D = -1.3, none (0%) of the toner is un-detachable, but the simulation does show that ~ 1% of the toner requires fields > 60 V/μm to detach.

The simulations indicate that the direction of the shift in the mean detachment field depends on how non-uniformly the toner is charged. For highly non-uniformly charged toner (θ<30) the mean detachment field tends to increase as magnitude of Q/D increases. The opposite trend shows up weakly in the simulations in figure 7 for θ=30. It is interesting to note that the experimental mean detachment field of EA spherical toner increased as the toner Q/D became larger (see figure 4). Although this consistent with the conclusion that the EA spheres are non-uniformly charged (despite their highly spherical shape), the experimentally observed shift is probably due to limitations in the model we used to estimate the peak field. It is possible that we have overestimated the experimental peak transfer field in the nip, since negatively charged toner that has transferred to the image receiving member at lower fields will tend to repel the toner still on the photoreceptor. Since this magnitude effect is hard to estimate due to the close proximity of the surfaces in the transfer zone, we did not include it in our calculation. Therefore if this effect is significant, the more highly charged the toner, the higher the overestimate of the applied field. This may account for much of the experimentally observed shift.

Table 3 the relationship between Q/D and tribo (Q/M)for a 6.2 μm diameter toner particle with a density if 1.24 g/cm^3.

[fC/um]	[uC/g]
Q/D	Tribo = Q/M
-0.3	-12
-0.5	-20
-0.7	-28
-0.9	-36
-1.1	-44
-1.3	-52.1
-1.5	-60.1

The high mean detachment field (>= 25 V/μm) observed for all of the toners is, however, strong evidence for highly non-uniformly charged toner. Simulations indicate that uniformly charged toner should typically detach at lower fields than we observed experimentally.

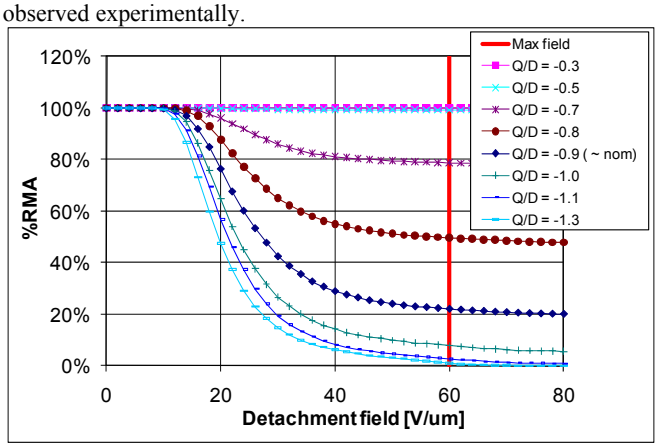

Figure 7 simulated fraction of residual toner as a function of toner charge Q/D

4. Conclusions

We have demonstrated that by *measuring* detachment field distributions, *modeling* adhesion forces, and *simulating* detachment field distributions based on those models, we can develop a much more detailed understanding of how key toner control factors impact detachment field distributions. This approach can be used to design toners and closed loop control schemes that could dramatically improve xerographic performance.

5. References

[1] C.A. DiRubio, A.M. Burry, A. DeCrescentis, Multi-color printing system and method for reducing the transfer field through closed-loop controls, US patent application 20100329702 (2010).

[2] J.Q. Feng and D.A. Hays, A finite element analysis of the electrostatic force on a uniformly charged dielectric sphere resting on a dielectric-coated electrode in a detaching electric field, IEEE Trans. Ind. Appl. 34 (1998), pg. 84-91.

[3] J.Q. Feng, E.A. Eklund, and D.A. Hays, Electric field detachment of a nonuniformly charged dielectric sphere on a dielectric-coated electrode, J. Electrost. 40 and 41 (1997), pg. 289-294.

[4] J.Q. Feng, and D.A. Hays, Theory of electric field detachment of charged toner particles in electrophotography, J. Imag. Sci. Technol. 44 (2000), pg. 19-25.

[5] Doug Kreckel, private communication.

6. Author Biography

Christopher A. DiRubio has worked on the development of new technologies and processes for both electrophotographic (xerographic) and phase change ink jet printing at Xerox Corporation for the past 16 years. He holds 15 US patents and 6 patent applications for his inventions, and is a design for lean six sigma black belt. In 1993 he received a Ph.D. in physics from Cornell University.